

# Stereo correspondence is optimized for large viewing distances

Graeme P. Phillipson<sup>1</sup> and Jenny C. A. Read<sup>2</sup>

<sup>1</sup>Neuroinformatics Doctoral Training Centre, Institute of Adaptive and Neural Computation, School of Informatics, Edinburgh University, Edinburgh, UK

<sup>2</sup>Institute of Neuroscience, Newcastle University, Henry Wellcome Building, Newcastle upon Tyne NE2 4HH, UK

**Keywords:** binocular vision, eye movements, human psychophysics, stereo correspondence, stereo vision, vertical disparity

## Abstract

Stereo '3D' vision depends on correctly matching up the differing images of objects seen by our two eyes. But vertical disparity between the retinal images changes with binocular eye posture, reflecting for example the different convergence angles required for different viewing distances. Thus, stereo correspondence must either dynamically adapt to take account of changes in viewing distance, or be hard-wired to perform best at one particular viewing distance. Here, using psychophysical experiments, we show for the first time that human stereo correspondence does not adapt to changes in physical viewing distance. We examine performance on a stereo correspondence task at a short viewing distance (30 cm) and show that performance is improved when we simulate the disparity pattern for viewing infinity, even though these disparities are impossible at the physical viewing distance. We estimate the vertical extent of the retinally fixed 'search zones' as  $< 0.6^\circ$  at  $14^\circ$  eccentricity, suggesting that most V1 neurons must be tuned to near-zero vertical disparity. We also show that performance on our stereo task at  $14^\circ$  eccentricity is affected by the pattern of vertical disparity beyond  $20^\circ$  eccentricity, even though this is irrelevant to the task. Performance is best when vertical disparities within and beyond  $20^\circ$  eccentricity both indicate the same convergence angle (even if not the physical angle), than when the pattern of vertical disparity across the visual field is globally inconsistent with any single convergence angle. This novel effect of the periphery may indicate cooperative interactions between disparity-selective neurons activated by the same eye postures.

## Introduction

The first step in 3D stereo vision is solving the stereo correspondence problem: correctly identifying pairs of points in the two eyes that are viewing the same object in space. Although retinas are 2D, stereo correspondence can in principle be made a 1D task. For any given point L in the left eye (Fig. 1A), the point that 'corresponds' to it, in the sense of being an image of the same object in space, must lie somewhere along the blue line in the right retina. Thus, in the space of 2D disparities, only disparities along a 1D 'epipolar line' are physically possible (green line in Fig. 1B). The trouble is that the location of the epipolar line depends on eye position, which is constantly changing. For example, as the eyes look up and down, they rotate about the line of sight, meaning that the epipolar lines rotate on the retina. To take account of this, the brain would have to use information about cyclorotation to direct the search for stereo correspondence along the appropriate epipolar lines.

Two recent papers have concluded that humans do not use oculomotor information in this way. van Ee & van Dam (2003) examined stereo correspondence in unconstrained stimuli, where the retinal images admit several different matches. They found that the

chosen match was close to horizontal on the retina, even when the eyes were cyclorotated so that the epipolar match was non-horizontal. Schreiber *et al.* (2001) used random-dot patterns to probe the limits at which stereo vision fails as the eyes cyclorotate. They demonstrated that the boundaries of the search zones remain fixed on the retina during cyclorotation.

However, Schreiber *et al.*'s elegant result regarding the 'boundaries' of search zones does not rule out shifts in sensitivity 'within' a search zone. In addition, previous work has only examined whether search zones shift in response to changes in cyclorotation, not gaze azimuth or convergence. Changes in cyclorotation are relatively small and relatively unusual, so it is understandable that the system should be hard-wired to perform optimally at zero cyclorotation, a natural 'center court position' (Tweed, 1997). Large changes in convergence, on the other hand, occur all the time, as we move our gaze between objects at different distances. Do stereo search zones remain fixed on the retina even under convergence changes? If so, stereo vision cannot be simultaneously optimized for all viewing distances. This raises the question of what viewing distance is chosen to be optimal, an answer that may depend on the ultimate purpose of stereo vision.

In this paper, we examine whether search zones shift in response to physical changes in convergence angle. We probe not just where stereo correspondence is possible, but where it is most sensitive. This enables us to answer: (i) whether stereo search zones shift their regions

Correspondence: Dr J. C. A. Read, as above.  
E-mail: j.c.a.read@ncl.ac.uk

Received 11 June 2010, revised 10 August 2010, accepted 26 August 2010

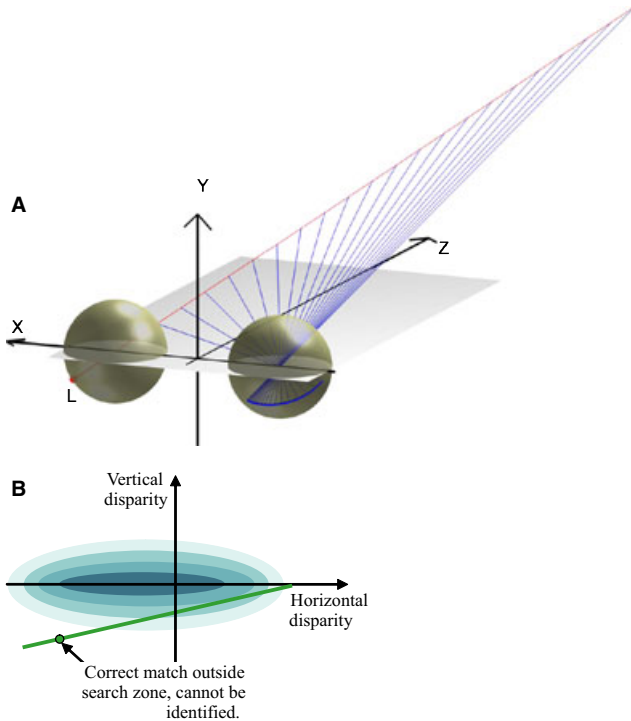


FIG. 1. Diagram illustrating the concept of a retinal search zone. These are based on Fig. 9 of Read *et al.* (2009). (A) The object *O*, which projects to the point *L* in the left eye, must lie somewhere along the red line in space, meaning that its image *R* in the right eye must lie along the blue ‘epipolar line’ in the right retina. (B) If we subtract off the position *L*, we can replot the epipolar line in disparity space (green line). The path of this line of physically possible disparities reflects both retinotopic position and the current binocular eye posture. If the stereo system searches for matches only within a ‘disparity search zone’ (shaded region), some physically possible matches will not be detected (if they fall outside the boundaries of the search zone), or will be detected less efficiently (if they fall far from the centre of the search zone).

of peak sensitivity to reflect physical convergence angle; (ii) if not, which viewing distance is optimal; and (iii) estimate the vertical extent of search zones.

## Materials and methods

### Task

The experimental set-up is sketched in Fig. 2. Subjects were briefly (192 ms) shown a pattern of small white dots randomly scattered on a black background. The dots all had zero horizontal disparity on the retina, except for a 4°-radius disk, centred at 14° eccentricity in one of the four quadrants, where the dots had a near disparity of  $-0.25^\circ$ . The task was to identify the quadrant containing the disk; a depth judgement was not required. Task difficulty was modulated by varying the binocular correlation *C* of the entire stimulus, not by changing disparity. That is, a fraction  $(1 - C)$  of dots were removed and replaced at new random locations, independently in the two eyes. This task was designed to probe the process of stereo correspondence itself (Cormack *et al.*, 1991), rather than how disparities are used once they have been detected. In between trials, subjects viewed a fixation cross,  $2.4^\circ \times 2.4^\circ$ , set to be directly in front of them at eye-height. The fixation cross was surrounded by horizontal and vertical Nonius lines each  $4.8^\circ$  long, and subjects were asked to ensure that both sets of Nonius lines remained aligned throughout. The stimuli were dynamic random-dot stereograms consisting of 12 successive 16-ms frames, each frame with the same parameters but a different pattern of random

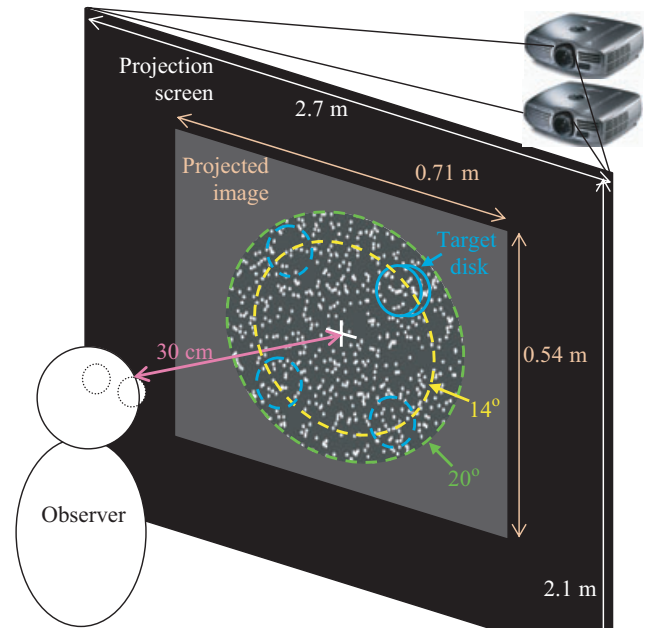


FIG. 2. Schematic of the stimulus. Coloured lines are there to mark locations and were not part of the experimental stimuli. The near-disparity target disk is shown here in the top-right quadrant (blue circle); the other three possible locations are marked with blue dashed lines. The yellow circle marks  $14^\circ$ , the eccentricity of the centre of the disk. The screen is frontoparallel to the observer, 30 cm in front of the eyes, with the fixation cross adjusted to the height of the eyes. This shows the ‘No-surround’ condition where the dot pattern extends out to  $20^\circ$  eccentricity. In the other conditions, the dot pattern filled the whole of the projected image (except at the edges, where due to the on-screen disparity a gap was left to avoid uncorrelated dots).

dots. The calculations used to generate the stimuli are described in detail below.

### Vertical-disparity conditions

The task was performed at a viewing distance of 30 cm, corresponding to a convergence angle of  $11^\circ$ . We compared performance under two conditions. First, in the ‘Consistent’ condition (indicated in the figures with cross-hatching ///), all dots had the correct epipolar disparities, i.e. disparities that were physically possible given the viewing distance. Due to the converged position of the eyes, the epipolar disparities have a vertical component on the retina. In the ‘Inconsistent’ condition (indicated with cross-hatching \\\), each dot was given a non-epipolar disparity designed to reduce the vertical component of its retinal disparity to zero. This simulates viewing infinity, i.e. zero convergence. To achieve this, dots were given a vertical disparity on the projection screen, whose magnitude and sign depended on the position of each dot and was carefully calculated, as described below, so as to null the vertical disparity on the retina. It is important to be clear here about the difference between retinal and on-screen disparities (see section below on definition of disparity). In the ‘Consistent’ condition, the stimulus dots had no on-screen vertical disparity, but did have retinal vertical disparity consistent with the physical convergence of  $11^\circ$ . In the ‘Inconsistent’ condition, dots had an on-screen vertical disparity, but no retinal vertical disparity, simulating a convergence of  $0^\circ$ , and inconsistent with the physical convergence of  $11^\circ$ . Example dot patterns and the disparity fields are shown in Fig. 3.

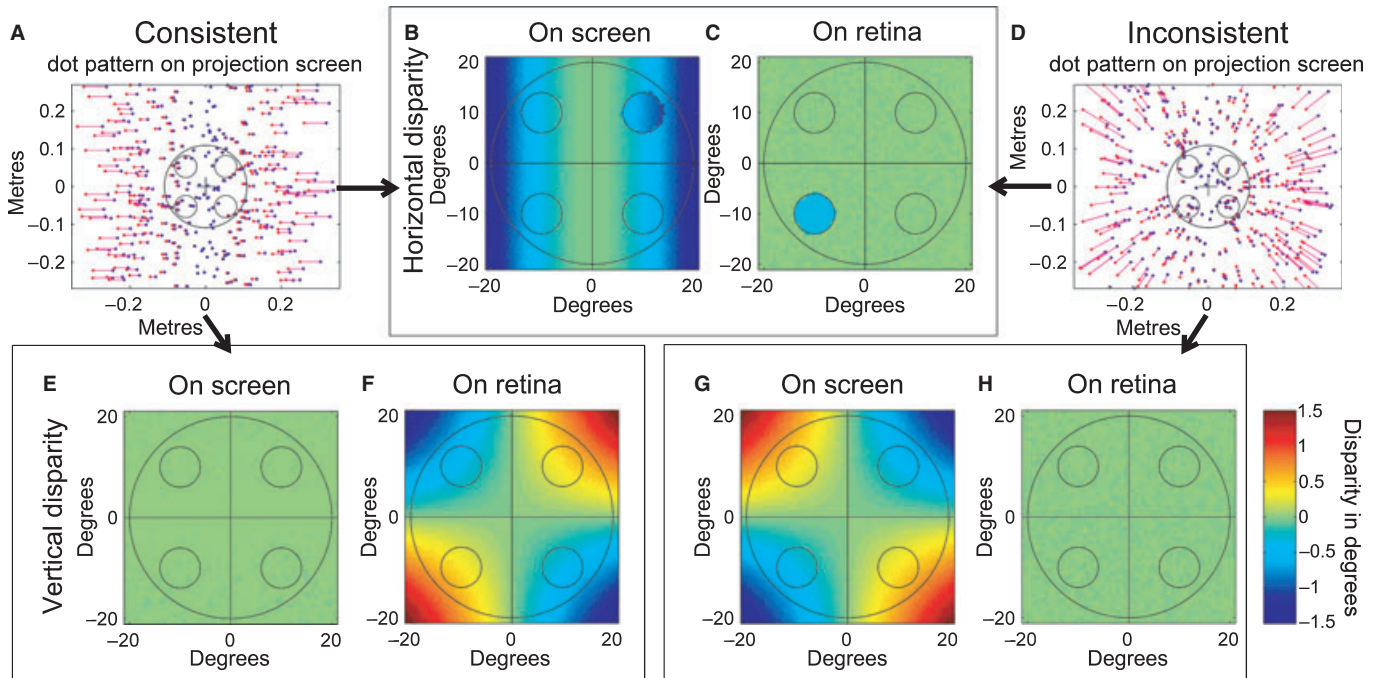


FIG. 3. ‘Consistent’ and ‘Inconsistent’ stimuli, and the disparity fields they produce. (A, D) Random-dot patterns on the projection screen. Horizontal and vertical axes are physical position in metres. Dots presented to the left (right) eye are shown in red (blue); corresponding dots are linked with a pink line. In the experiments all dots were white on a black background, and the linking lines were not present. The 20° circle and the four possible target locations are marked with black circles; the circles were not present in the experiments. (A) ‘Consistent’ condition: dots have no vertical disparity on the screen (E), so their vertical disparity on the retina (F) is epipolar, i.e. appropriate for the physical convergence of 11°. (D) ‘Inconsistent’ condition: dots have vertical disparities of up to several degrees on the screen (G), chosen so that they produce no vertical disparity on the retina (H), as would normally occur for zero convergence. In both ‘Consistent’ and ‘Inconsistent’ conditions, stimuli have zero retinal horizontal disparity (B and C) except in the disparate target disk. Dots therefore lie on the horopter, the region of maximum stereoacuity. Retinal horizontal/vertical disparities are calculated in azimuth/elevation-longitude coordinates. In these examples, the stimulus binocular correlation is 100%.

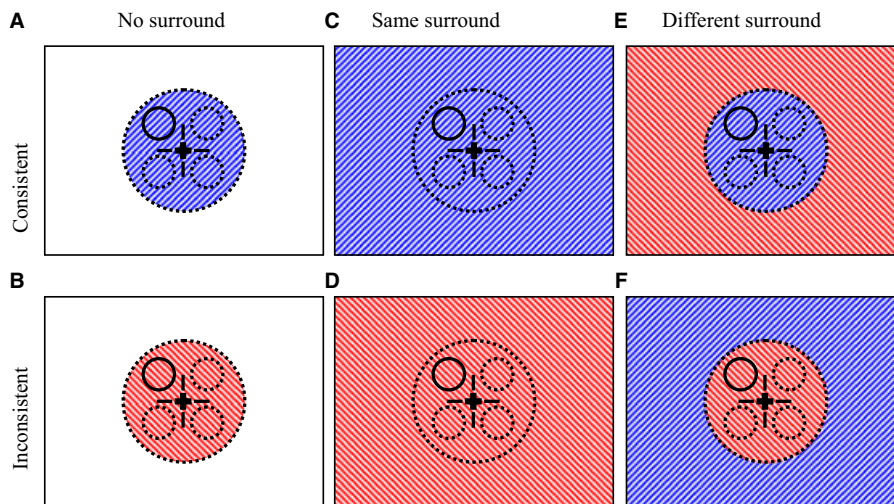


FIG. 4. Schematic summarizing the six types of stimuli. The small black circles mark the four possible positions of the disparate target; only one of these is occupied on any trial. The larger dotted circle marks 20° eccentricity. The shading indicates whether the vertical disparity in that region is appropriate for the physical convergence (‘Consistent’ vertical disparity, ///) or for zero convergence (‘Inconsistent’ vertical disparity, \\\\). Stimuli are labelled ‘Consistent’ or ‘Inconsistent’ according to the vertical-disparity pattern within 20° eccentricity. The circle symbols in Figs 5 and S1 show data from stimuli in the top row (‘Consistent’ condition); the squares show data from stimuli in the bottom row (‘Inconsistent’).

#### Surround conditions

In the ‘No-surround’ condition (Figs 2 and 4A and B), the random-dot pattern occupied a circle of radius 20° centred on the fixation cross. We also examined the effect of presenting more dots in the remaining area of the projection screen. These surround dots always had zero horizontal retinal disparity, while their vertical retinal disparity varied

depending on the condition. In the ‘Same-surround’ condition (Fig. 4C and D), we simply extended the pattern out across the whole screen. In the ‘Different-surround’ condition (Fig 4E and F), we calculated vertical disparities based on different eye postures for the central 20° and for the surrounding region. Thus, in the ‘Consistent’/‘Different-surround’ condition, the central 20° had vertical

disparities consistent with the physical convergence of 11°, while the surrounding region had vertical disparities appropriate for 0° convergence. In the ‘Inconsistent’/‘Different-surround’ condition, the central 20° had vertical disparities appropriate for 0° convergence, while the surround had vertical disparities consistent with the physical convergence of 11°.

### Equipment

Each eye’s image was presented on a separate F2sx+ Projection Design DLP projector with a resolution of 1400 × 1050 pixels and a refresh rate of 60 Hz. Polarizing filters ensured that each eye saw only one projector’s image, viewed on a frontoparallel rear projection screen. Interocular cross-talk was < 1%. Gamma-correction and image alignment was as described previously (Serrano-Pedraza & Read, 2009). Observers used a head and chin rest, which held their eyes at the same height as the fixation cross, at a viewing distance of 30 cm. The fixation cross was midway between the observers’ eyes. Laser cross-lines, projected at vertical and horizontal with respect to gravity (Autocross Laser 2, Laserliner), were used to check alignment. The projected image was 71 cm wide × 54 cm high (100° × 84°), while the projection screen on which it appeared was 270 × 210 cm (155° × 148°), forming one wall of the room in which observers sat. White dots had a luminance of 140 cd/m<sup>2</sup>, and the black background of the projected image was 2 cd/m<sup>2</sup>, both measured through the polarizing glasses. Experiments were performed in darkness to minimize any disparity information from the surroundings. Stimuli were generated in MATLAB (The Mathworks, Natick, MA, USA; <http://www.mathworks.com>) using the Psychophysics Toolbox (Brainard, 1997; Pelli, 1997).

### Data analysis

Performance as a function of binocular correlation for a given stimulus was described by a cumulative-Weibull function,

$$P_{D,S}(C) = 0.25 + 0.75\{1 - \exp[-(r_{D,S}C)^k]\}, \quad (1)$$

where  $P$  is the proportion of correct answers (0.25 is chance) and  $C$  is the stimulus binocular correlation. Here and subsequently in the paper, the indices  $D,S$  indicate the stimulus condition: the index  $D$  indicates the vertical-disparity configuration and can take values ‘Consistent’ or ‘Inconsistent’, while the index  $S$  indicates the surround configuration and can take values ‘No-surround’, ‘Same-surround’ or ‘Different-surround’. The seven parameters  $r_{D,S}$  and  $\kappa$  were fit to all six stimulus conditions simultaneously (at least 30 data-points for each subject) by the method of maximum likelihood assuming simple binomial statistics.

### Subjects

The subjects were eight graduate students, four male and four female, aged between 19 and 30 years. G.P.P. is an author; the others were unaware of the purpose of the experiment and most had no previous experience of psychophysics. Two potential subjects were rejected in initial screening because they could not reach threshold performance on this difficult brief-duration, peripheral-vision stereo task. Subjects each performed at least four blocks of 150 trials (five repetitions of five different correlation levels, two conditions, three experiments). Although the ‘Consistent/Inconsistent’ conditions and Experiments

1–3 are described separately in the text for clarity, during data collection all six combinations were randomly interleaved from trial to trial.

### Ethics

This project was approved by Newcastle University Faculty of Medical Sciences Ethics Committee, and conformed to the Code of Ethics of the World Medical Association (Declaration of Helsinki).

### Definition of disparity

The term ‘vertical disparity’ has been used with many different meanings in the literature; see Read *et al.* (2009) for a detailed discussion. In this paper, ‘on-screen vertical disparity’ means that the left and right images were offset vertically on the projection screen, i.e. disparity in optic-array Helmholtz elevation coordinates. This is always non-epipolar, producing retinal images that are inconsistent with the physical eye position. By ‘retinal vertical disparity’, we mean a disparity in the elevation-longitude coordinate,  $\eta$ , on the two retinas (similarly retinal horizontal disparity means a disparity in azimuth-longitude,  $\alpha$ ). Apart from the fovea, all retinal locations can experience elevation-longitude disparities during natural viewing. The elevation-longitude retinal coordinate system is particularly convenient for describing our experiment, because we simulate the disparity field produced when the eyes are in primary position (zero elevation, zero convergence, fixating a point on the midline at infinity). Under these conditions, elevation-longitude disparity is zero everywhere on the retina, irrespective of the visual scene. The stimuli and results of our paper are independent of the retinal coordinate system chosen to describe them, but clearly our quantitative statements regarding vertical disparities are valid only in the specified coordinate system.

### Disparity calculations

The target disk is centred on retinal azimuth-longitude  $|\alpha| = 10^\circ$ , elevation-longitude  $|\eta| = 10^\circ$ , and has a radius of  $4^\circ$ . Its minimum eccentricity is thus  $\xi = 10^\circ$ , occurring at  $|\alpha| = 7.2^\circ$ ,  $|\eta| = 7.2^\circ$ , and its maximum is  $18^\circ$ . For fixation on the midline, the vertical disparity  $V$  experienced at retinal location  $(\alpha, \eta)$  depends only on the vergence angle  $H$ , not on the visual scene. From eqn (18) of Read *et al.* (2009), the vertical disparity in elevation-longitude retinal coordinates is  $V \approx H \sin \eta \cos \eta \tan \alpha$ . Thus, in natural viewing at 30 cm ( $H = 11.5^\circ$ , assuming an inter-pupillary distance of 6.02 cm for purposes of exposition), the vertical disparity at the centre of the target is  $V = 0.35^\circ$ , and at the most foveal point in the target, it is  $V = 0.18^\circ$ . (The magnitudes are the same for all target locations; the sign depends on the quadrant.) In natural viewing at infinity, all vertical disparities are zero.

These calculations assume that the observers’ eyes were not cyclorotated. Because we did not measure primary position for our observers, we do not know whether their eyes were elevated or depressed a few degrees from primary position. Much previous work on binocular eye movements, summarized in ‘L2’ or the binocularly extended version of Listing’s law (Mok *et al.*, 1992; Tweed, 1997; Schreiber *et al.*, 2001), indicates that there is no overall cyclotorsion when the eyes are fixating the mid-sagittal plane. For the idealized  $\mu = 0.25$  version of L2, no cyclovergence occurs either, even if the elevation is non-zero. For other values of  $\mu$ , cyclovergence is possible if the elevation is non-zero. Thus, we cannot rule out small amounts of cyclovergence, below an estimated upper bound of 0.07°.

However, this would have opposite effects on vertical disparity in each visual hemifield. Thus, in the analysis below, small amounts of cyclovergence would contribute additional variability, not a systematic error.

### Calculating dot positions

Stimulus disparity, dot-density, etc. were all specified on the retina rather than the screen. We use azimuth-longitude  $\alpha$ /elevation-longitude  $\eta$  retinal coordinates (Read *et al.*, 2009). Dots were scattered at constant density on the visual sphere, resulting in small changes in dot density as a function of position on the frontoparallel projection screen. The dot density was 5157 dots per steradian (on average one dot per square degree of visual angle). To generate the initial dot positions, azimuth-longitude,  $\alpha$ , was picked uniformly from  $[-\pi/4, +\pi/4]$ , and the sine of elevation-latitude,  $\sin(\lambda)$ , was picked uniformly from  $[-1, 1]$ . Elevation-longitude,  $\eta$ , was then given by  $\eta = \arctan(\tan(\lambda)/\cos(\alpha))$ .

Dots within the circular target are then given an azimuth-longitude disparity of  $0.25^\circ$  (crossed). The target is centred on one of the four possible positions  $\alpha_0 = \pm 10^\circ$ ,  $\eta_0 = \pm 10^\circ$ . Dots satisfying  $(\alpha - \alpha_0)^2 + (\eta - \eta_0)^2 < (4^\circ)^2$  had their value of  $\alpha$  reduced by  $0.125^\circ$  in the left retina and increased by  $0.125^\circ$  in the right retina, resulting in separate values  $\alpha_L$  and  $\alpha_R$ . Thus, at this point, all dots have zero vertical disparity on the retina, most dots also have zero horizontal disparity on the retina, while dots within the target disk have a near-horizontal disparity of  $0.25^\circ$  on the retina. Thus, at present the stimulus is appropriate for the ‘Inconsistent’ condition.

To obtain stimuli appropriate for the ‘Consistent’ condition, we need to adjust each dot’s retinal vertical disparity to the value that would be obtained for natural viewing at 30 cm. This will make the disparities geometrically correct (‘epipolar’) for the physical viewing distance. To do this, we used a convenient result of epipolar geometry: the fact that epipolar disparities correspond to purely horizontal shifts on a frontoparallel projection screen. Imagine a virtual projection screen at a viewing distance  $Z_V$ . To obtain epipolar disparities appropriate to viewing distance  $Z_V$ , each dot must have the same vertical  $Y$ -coordinate on the screen in both eyes. At the moment, to obtain retinal images at  $(\alpha_L, \eta)$  and  $(\alpha_R, \eta)$ , dots must have screen-coordinates given by:

$$\begin{aligned} \frac{X_{VL}}{Z_V} &= -\frac{\tan \alpha_L \cdot \sec \theta_V}{(\cos \theta_V - \sin \theta_V \cdot \tan \alpha_L)}, \\ \frac{X_{VR}}{Z_V} &= -\frac{\tan \alpha_R \cdot \sec \theta_V}{(\cos \theta_V + \sin \theta_V \cdot \tan \alpha_R)}, \\ \frac{Y_{VL}}{Z_V} &= -\tan \eta \left( \sec \theta_V - \frac{X_{VL}}{Z_V} \sin \theta_V \right), \\ \frac{Y_{VR}}{Z_V} &= -\tan \eta \left( \sec \theta_V + \frac{X_{VR}}{Z_V} \sin \theta_V \right) \end{aligned}$$

where  $\theta_V = \arctan(J/Z_V)$  is half the vergence angle required to fixate the screen,  $J$  is half the inter-pupillary distance (measured individually for each observer), and  $X_V$  and  $Y_V$  are horizontal and vertical distance coordinates on the virtual screen. For the ‘Inconsistent’ condition,  $Z_V = \infty$  and  $\theta_V = 0^\circ$ . Thus, in this case, these equations reduce to  $X_{VL}/Z_V = -\tan \alpha_L$ ,  $X_{VR}/Z_V = -\tan \alpha_R$ ,  $Y_{VL} = Y_{VR} = -Z_V \tan \eta$ . Because  $Y_{VL} = Y_{VR}$ , the retinal dots are already epipolar for infinite viewing distance. For the ‘Consistent’ condition,  $Z_V = 30$  cm and  $\theta_V$  is  $5.7^\circ$  for an inter-pupillary distance of 6 cm. Thus, in general for the ‘Consistent’ condition,  $Y_{VL}$  is not equal to  $Y_{VR}$ . To make

the disparities epipolar for a viewing distance of 30 cm, we need to shift the dots vertically so that left- and right-eye dots are at the same vertical position on the screen, e.g. at  $(Y_{VL} + Y_{VR})/2$ . As a result, the dots no longer project to the same elevation on the retina, but to different elevations in left and right eyes, depending on their location in the visual field:

$$\begin{aligned} \tan \eta_L &= -\left( \frac{Y_{VL} + Y_{VR}}{2Z_V} \right) \frac{\cos \theta_V}{1 - (X_{VL}/Z_V) \cos \theta_V \sin \theta_V} \\ \tan \eta_R &= -\left( \frac{Y_{VL} + Y_{VR}}{2Z_V} \right) \frac{\cos \theta_V}{1 + (X_{VR}/Z_V) \cos \theta_V \sin \theta_V} \end{aligned}$$

After all this, we have a set of dot positions on the two retinas,  $(\alpha_L, \eta_L)$  and  $(\alpha_R, \eta_R)$ , whose disparities have zero horizontal component (apart from at the target location) and are epipolar for viewing distance  $Z_V$ . We now have to work out where to plot dots on our physical projection screen, located at viewing distance  $Z_P = 30$  cm, in order to produce retinal images at the desired locations:

$$\begin{aligned} X_{PL} &= -\frac{Z_P \tan \alpha_L \sec \theta_P}{\cos \theta_P - \sin \theta_P \tan \alpha_L}, & X_{PR} &= -\frac{Z_P \tan \alpha_R \sec \theta_P}{\cos \theta_P + \sin \theta_P \tan \alpha_R} \\ Y_{PL} &= -(\tan \eta_L)(Z_P \sec \theta_P - X_{PL} \sin \theta_P), \\ Y_{PR} &= -(\tan \eta_R)(Z_P \sec \theta_P + X_{PR} \sin \theta_P) \end{aligned}$$

In the ‘Consistent’ condition, the retinal vertical disparities are set appropriately to the physical viewing distance ( $\theta_V = \theta_P$ ), which means there are no vertical disparities on the screen ( $Y_{PL} = Y_{PR}$ ). In the ‘Inconsistent’ condition, the retinal vertical disparities are set inappropriately ( $\theta_V = 0$ ), and there are vertical disparities on the screen ( $Y_{PL} \neq Y_{PR}$ ). Figure 3 shows example stimuli as they appeared on the projection screen for the ‘Same-surround’ condition, (Fig. 3A) ‘Consistent’ condition and (Fig. 3B) ‘Inconsistent’ condition. The on-screen vertical disparities are clearly visible in Fig. 3B.

## Results

Figure 5 shows a complete set of data for one of our eight subjects, for the six stimulus conditions. In each condition, performance rises from chance when the stimulus is completely uncorrelated, to near-perfect when the stimulus was perfectly correlated. But, strikingly, performance was always better for the ‘Inconsistent’ condition (squares in Fig. 5), even though the vertical disparities here are correct for zero convergence, in conflict with the physical convergence of  $11^\circ$ . The extent of the difference varied across subjects, but no subjects performed better on the ‘Consistent’ condition. Subjects were better at detecting the target disk when the retinal vertical disparity at its centre was  $0.00^\circ$  than when it was  $0.35^\circ$ , even though the physical eye posture means that only the latter is physically possible.

We can immediately deduce that sensed convergence plays little or no role in guiding stereo correspondence along the right epipolar lines. Zero vertical disparity, indicating a fixation distance of infinity, is as far away as possible from the highly converged viewing angle actually adopted by subjects. Yet subjects still performed better for zero vertical disparity. We conclude that not only the boundary of the search zone (Schreiber *et al.*, 2001), but also its region of maximal sensitivity, is fixed on the retina, and does not shift to reflect physical convergence. Furthermore, this region of maximal sensitivity must be centred vertically nearer to  $0^\circ$  than  $0.35^\circ$ .

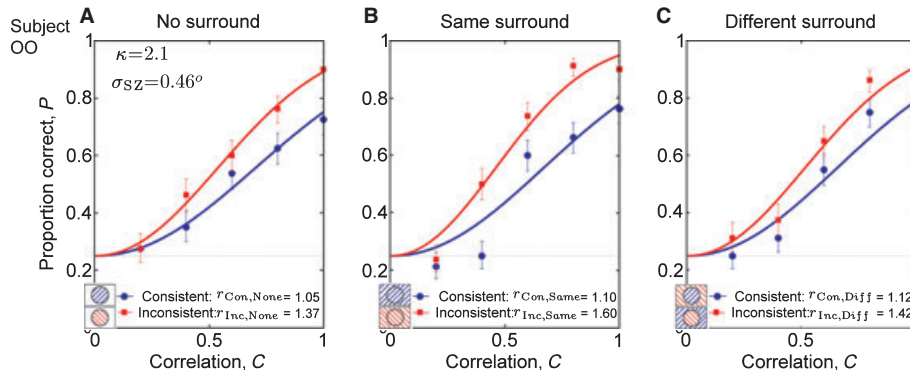


FIG. 5. Complete results for an example subject, O.O. Symbols represent the proportion of trials in which the subject correctly identified the quadrant containing the target disk, as a function of the binocular correlation of the stimulus. Error-bars show 68% confidence intervals assuming simple binomial statistics. Circles show results for the ‘Consistent’ condition: when the central 20° of the visual field contained vertical disparities consistent with the physical convergence of 11°. Squares show results for the ‘Inconsistent’ condition: when the central 20° contained vertical disparities indicating zero convergence. In each case, performance is better on the ‘Inconsistent’ condition. The three panels (A)–(C) are for the three different surround conditions. The icons in the legend are as in Fig. 4. (A) ‘No-surround’ (screen was black beyond 20° eccentricity). (B) ‘Same-surround’ (dots extended beyond 20° eccentricity, with vertical disparities calculated for the same convergence as in the centre). (C) ‘Different-surround’ (‘Consistent’ condition: vertical disparities in the centre indicated the physical convergence, those in the surround indicated zero convergence; ‘Inconsistent’ condition: vertical disparities in the centre indicated zero convergence, those in the surround indicated the physical convergence). The curves show the results of fitting cumulative-Weibull functions simultaneously to all data (Eqn 1); parameters  $r$  are fit for each condition separately and are given in the legend for each panel; parameter  $\kappa$  is fit to all data and is given in the first panel;  $\sigma_{SZ}$  is the estimated vertical extent of the subject’s search zones.

A possible disparity search zone is sketched in Fig. 6. The shading represents the sensitivity of the search zone. The search zone is shown as highly elongated horizontally, reflecting the psychophysical result that depth perception tolerates a wider range of horizontal than vertical disparities (Duwaer & van den Brink, 1982; Prazdny, 1985; Stevenson & Schor, 1997), the physiological distribution of preferred disparity tuning in V1 (Cumming, 2002), the horizontally elongated disparity tuning surfaces of V1 neurons (Cumming, 2002), and the ecological distribution of disparity (Read & Cumming, 2004; Hibbard, 2007; Liu *et al.*, 2008). It is shown as centred on zero horizontal disparity, reflecting the greater stereoacuity found at the geometrical horopter (Blakemore, 1970). Our results imply that it must also be centred near-zero vertical disparity, as performance is better for a vertical disparity of 0° (square) than 0.35° (circle).

The stereo energy model has been developed to explain the response properties of V1 disparity-selective neurons (Ohzawa *et al.*,

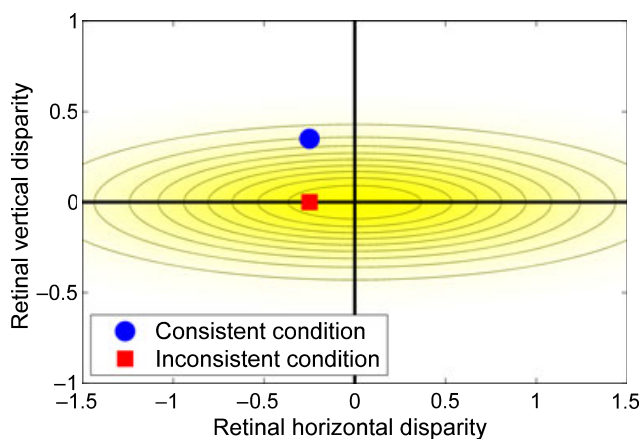


FIG. 6. Sketch of a search zone. The axes show horizontal and vertical retinal disparity, in degrees. The shading/contour lines show the sensitivity of the stereo system as a function of 2D disparity. The symbols show the 2D disparity of our stimulus, at the centre of the target disk. Because performance was better on the ‘Inconsistent’ condition (square), we conclude that the search zone is centred near-zero vertical disparity.

1990; Ohzawa, 1998). In models of this kind, a mismatch between the vertical disparity of the stimulus and the vertical disparity to which the neuron is maximally sensitive is equivalent to a reduction in the binocular correlation of the stimulus (Read & Cumming, 2006). A mismatch of  $\Delta V$  reduces the effective binocular correlation by a factor of  $\exp(-\Delta V^2/4\sigma_{RF}^2)$ , where  $\sigma_{RF}$  is the standard deviation of the neuron’s monocular receptive fields. Motivated by this, we examine whether our subjects’ results can be expressed as a change in the effective binocular correlation.

We fitted all six psychometric functions with a cumulative-Weibull function (see Materials and methods). The parameter  $\kappa$ , which controls the shape of the function, was kept constant for all six conditions. The parameter  $r$ , which scales the stimulus binocular correlation, was fit separately for each condition, resulting in a total of seven parameters for the six curves. This model therefore assumes that the difference in performance between the different conditions can be expressed as a multiplicative change in the effective binocular correlation of the stimulus. The model produced good fits for each subject, explaining over 90% of variance for all eight subjects, and over 95% for six out of eight. This confirms that the difference in performance between the different conditions can be summarized by a ‘gain change’ in stimulus correlation.

Performance was almost always best in the ‘Inconsistent’/‘Same-surround’ condition. To compare the effects across subjects, we first normalized each subject’s  $r$ -values by their value for this condition. This ratio,  $r_{D,S}/r_{Inc,Same}$ , represents the factor by which the effective stimulus correlation is reduced in the  $D,S$  condition relative to the ‘Inconsistent’/‘Same-surround’ condition. Lower values of the ratio thus indicate worse performance. The filled symbols in Fig. 7 summarize this ratio, averaged over all subjects, for the six conditions (the open symbols are fits, discussed below). We see that both surround configuration ( $S = \text{None/Same/Different}$ ; see Fig. 4) and vertical-disparity pattern ( $D = \text{Consistent/Inconsistent}$  with physical convergence) affect performance. Performance is worst in the ‘Different-surround’ configuration, where dots inside and outside 20° indicated conflicting eye positions, best in the ‘Same-surround’, and intermediate when there is ‘No-surround’. Additionally, for each surround configuration, performance is worse in the ‘Consistent’ than

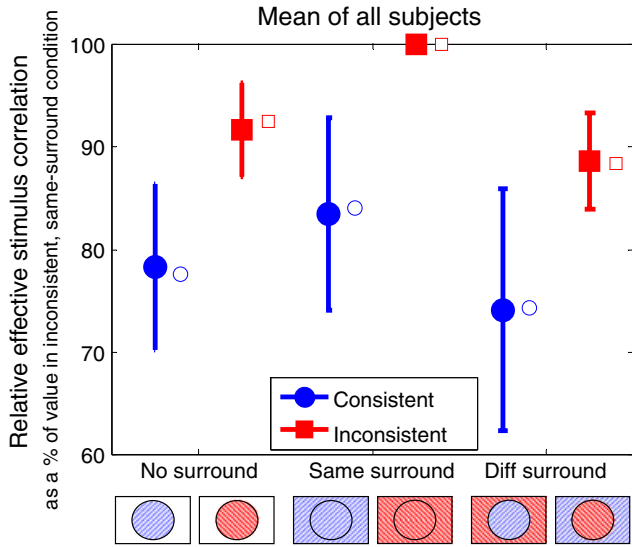


FIG. 7. Summary of results for all eight subjects. Filled symbols show the geometric mean value, averaged across subjects, of  $r_{D,S}/r_{Inc,Same}$ . This is the factor by which the effective binocular correlation is reduced in the  $D,S$  condition compared with the ‘Inconsistent’/‘Same-surround’ condition where performance was best. Circles show results for  $D = \text{Consistent}$ , squares for  $D = \text{Inconsistent}$ . The three pairs of points show results for  $S = \text{‘No-surround’}$ , ‘Same-surround’ and ‘Different-surround’. The fourth data-point is 100% by definition. Error-bars show  $\pm 1$  standard deviation of the results for the eight subjects individually. Open symbols show the results of fitting the model of Eqn 2.

the ‘Inconsistent’ vertical-disparity condition. A two-way ANOVA on  $\ln(r_{D,S}/r_{Inc,Same})$  indicated that both vertical disparity  $D$  and surround configuration  $S$  had a significant effect on performance ( $P = 5 \times 10^{-6}$  for vertical disparity,  $P = 0.002$  for surround), but that their interaction was not significant.

Thus, Fig. 7 shows both vertical-disparity conditions and surround conditions affect performance. The effect of vertical disparity is consistent with the idea of retinally fixed search zones, as developed by Schreiber *et al.* (2001). Suppose that the search zone is centred on zero retinal vertical disparity, as in Fig. 6. Then a non-zero retinal vertical disparity  $V$  will reduce the effective binocular correlation of the stimulus (Read & Cumming, 2006). This explains why performance is better in the ‘Inconsistent’ condition, when  $V$  is zero, than in the ‘Consistent’ condition, when  $V = 0.35^\circ$ .

Search zones are necessarily local; their extent reflects the range of perceptible disparities, a few degrees at most. Yet, our results also clearly show that vertical disparities from many degrees away have a measurable effect on performance. Adding a surround whose vertical disparities indicate the same eye posture as the centre significantly boosts performance, even if the eye posture indicated by these vertical disparities is not the physical eye posture adopted by the observer ( $r_{D,Same} > r_{D,None}$  for both values of  $D$ ). If, however, the vertical disparities in the surround indicate a different eye posture from those in the centre, then performance is reduced ( $r_{D,Diff} < r_{D,None}$ ). Comparing the ‘No-surround’ condition with the ‘Same-’/‘Different-surround’ conditions is arguably problematic, as these stimuli have a number of gross differences, for example their total luminance or in the amount of relative horizontal disparity information provided by the larger stimulus. We can avoid this by comparing the ‘Same-’ vs. ‘Different-surround’ conditions. These differ only in the pattern of vertical disparities beyond  $20^\circ$  eccentricity: the retinal horizontal disparity, dot density, number of dots, etc. are all identical. Nevertheless, these two surround configurations produce very different

results, with  $r_{D,Diff} < r_{D,Same}$  for both vertical-disparity conditions  $D$ . This shows that the pattern of vertical disparities in the task-irrelevant far periphery can measurably affect performance on a stereo correspondence task.

This effect of the surround can be described as a multiplicative gain operating on the effective correlation of the stimulus. Our results are described very well by a model of the form

$$C_{D,S} = C_{stim} G_S \exp(-V_D^2/2\sigma_{SZ}^2) \quad (2)$$

Equation 2 describes how the effective correlation experienced by the stereo system,  $C_{D,S}$ , is reduced below that available in the stimulus,  $C_{stim}$ , by two factors. The exponential term models the effect of the stimulus vertical disparity,  $V_D$ , as discussed above, where  $V_{Inc}$  is  $0^\circ$  everywhere and  $V_{Con}$  is  $0.35^\circ$  at the centre of the target disk. The search zone is assumed to be vertically centred on zero, and the parameter  $\sigma_{SZ}$  represents its vertical extent. The gain  $G_S$  models the effect of the surround. Because we are only trying to model the relative changes in effective stimulus correlation between conditions, we can set  $G_{None} = 1$  without loss of generality.  $G_{Same}$  then represents the beneficial effect of extending the stimulus beyond  $20^\circ$ , when the vertical disparities indicate the same eye posture as elsewhere in the visual field. Conversely,  $G_{Diff}$  represents the damaging effect when vertical disparities beyond  $20^\circ$  indicate a different eye posture. Our data suggest that although  $G_S$  depends critically on whether the vertical-disparity field is globally consistent with a single eye posture, it is independent of whether that eye posture is the one actually adopted (i.e.  $G_S$  is independent of  $D$ ).

The open symbols in Fig. 7 show the results of fitting Eqn 2 to data-points shown with filled symbols. The three model parameters are fitted to five data-points (as one point is 1 by definition), to obtain  $\sigma_{SZ} = 0.58^\circ$ ,  $G_{Same} = 1.08$  and  $G_{Diff} = 0.96$ . Although the small number of data-points relative to parameters makes this good agreement less impressive, Eqn 2 does do a very good job of capturing how vertical disparity and stimulus configuration alter the effective stimulus correlation. Supporting Information Fig. S2 shows that this model also works well for all eight subjects individually. There is some variation in the value of  $\sigma_{SZ}$  estimated for different subjects, ranging from  $0.40$  to  $1.1^\circ$ . The value of  $G_{Same} < G_{Diff}$  for every subject. Fitted parameters for all eight subjects are given in Supporting Information Table S1.

An important feature of Eqn 2 is that, because surround configuration enters only through a multiplicative gain, the reduction in stimulus correlation between the two vertical-disparity conditions must be independent of surround configuration:

$$r_{Con,S}/r_{Inc,S} = \exp(-(0.35^\circ)^2/2\sigma_{SZ}^2) \text{ for all } S. \quad (3)$$

This is the factor by which the effective binocular correlation in the ‘Consistent’ condition is reduced relative to that in the ‘Inconsistent’ condition, i.e. how much worse for stereo vision a convergence angle of  $11^\circ$  is compared with a convergence angle of  $0^\circ$ . On average over all subjects and surround conditions, this ratio is 0.84, leading to the estimate of  $0.58^\circ$  for  $\sigma_{SZ}$ .

Because this ratio is central to our conclusions, we examine it further in Fig. 8. This plots the ratio  $r_{Con,S}/r_{Inc,S}$  for each subject; the different symbols show results for the three different surround configurations  $S$ . In the final column, the results are shown averaged over all eight subjects. The ratio  $r_{Con,S}/r_{Inc,S}$  is  $< 1$  in 23 out of 24 experiments (eight subjects  $\times$  three surround conditions). At a

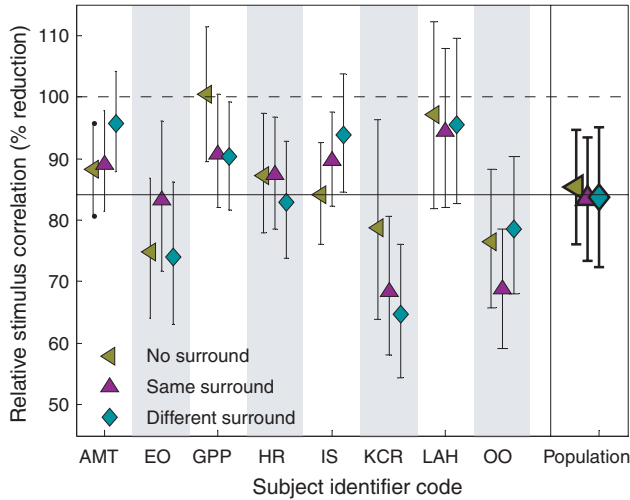


Fig. 8. Breakdown of results for individual subjects, showing that performance is reduced in the ‘Consistent’ condition compared with the ‘Inconsistent’ condition. Symbols show  $r_{\text{Con},S}/r_{\text{Inc},S}$ , the factor by which the effective binocular correlation is reduced in the ‘Consistent’ condition compared with the ‘Inconsistent’ condition, for surround condition  $S$ , where  $S$  can be ‘No-surround’ (◄), ‘Same-surround’ (▲) or ‘Different-surround’ (◆), see Fig. 4. Error-bars for individual subjects show the 95% confidence intervals obtained by boot-strap resampling. The final column, labelled ‘Population’, shows the population results averaged across subjects; error-bars here show  $\pm 1$  standard deviation of the results for individual subjects. The solid horizontal line shows the geometric mean over all subjects and surround conditions, while the dashed line marks 100%, i.e. no difference between the ‘Consistent’ and ‘Inconsistent’ conditions.

population level, this already enables us to reject the null hypothesis that performance is the same in the ‘Consistent’ and ‘Inconsistent’ conditions [ $P < 10^{-5}$ , two-sided sign test on  $\ln(r_{\text{Con},S}/r_{\text{Inc},S})$ ]. At the level of individual experiments,  $r_{\text{Con},S}/r_{\text{Inc},S}$  is significantly  $< 1$  at the 5% level in 17/24 experiments (two-sided test using 95% confidence intervals from bootstrap resampling). Thus, our conclusion that stereo correspondence is optimized for long viewing distances is robust.

As Eqn 3 shows, our model states that the ratio  $r_{\text{Con},S}/r_{\text{Inc},S}$  is independent of surround  $S$ . Figure 8 confirms that this is true for individual subjects as well as for the averaged population results shown in Fig. 7. Within each subject, the small differences between the three  $S$  configurations never reach significance at the 5% level, and there is no consistent effect of surround across subjects, suggesting that this variation merely reflects random variation in performance. Thus, for each subject, it is possible to define a unique ratio  $r_{\text{Con}}/r_{\text{Inc}}$ , independent of surround configuration. It is this ratio that is fitted by the model parameter  $\sigma_{\text{SZ}}$ .

The simple model put forward in Eqn 2 is not unique, but our data do not allow us to discriminate more closely between different models. In particular, Eqn 2 assumes the search zone is centred on a vertical disparity of  $0^\circ$ , as sketched in Fig. 6, i.e. that stereo vision is optimized for a convergence angle of  $H_{\text{opt}} = 0^\circ$ . Really, our data only allow us to conclude that stereo vision must be optimized for convergences that are nearer to  $0^\circ$  than to the physical convergence of  $H_{\text{phys}} = 11.5^\circ$ , i.e. that  $H_{\text{opt}} < 5.7^\circ$ . Any subject with  $H_{\text{opt}} > 5.7^\circ$  would show impaired performance in the ‘Inconsistent’ condition ( $r_{\text{Con},S}/r_{\text{Inc},S} > 1$ ), and this was never observed.

It can be shown that the values of  $\sigma_{\text{SZ}}$  estimated above under the assumption of zero  $H_{\text{opt}}$  are in fact upper bounds. If the optimal convergence is  $H_{\text{opt}}$ , then at the centre of the target disk, search zones will be centred on vertical disparity  $V_{\text{cen}} = 0.03H_{\text{opt}}$ . Generalizing Eqn 3 to account for this, we obtain

$$r_{\text{Con},S}/r_{\text{Inc},S} = \exp(-[V_{\text{cen}} - 0.35^\circ]^2/2\sigma_{\text{SZ}}^2) / \exp(-V_{\text{cen}}^2/2\sigma_{\text{SZ}}^2)$$

As Fig. 8 shows, the mean value of this ratio over all subjects and surround conditions is 0.84. Taking this together with  $V_{\text{cen}} = 0.03H_{\text{opt}}$  leads to

$$\sigma_{\text{SZ}} = \sqrt{0.344 - 0.060\theta_{\text{opt}}}, \quad (4)$$

where all quantities are in degrees. Thus, our results assuming  $H_{\text{opt}} = 0$  are upper bounds. Equally good fits could be provided with somewhat larger values of  $H_{\text{opt}}$ , provided  $\sigma_{\text{SZ}}$  was reduced accordingly, which is why it is not possible to extract  $H_{\text{opt}}$  from our data. This would require further experiments that simulated a range of different convergence angles in order to see where performance peaks.

Variation in the optimal convergence angle likely explains some of the variation in fitted  $\sigma_{\text{SZ}}$  between subjects. Subjects who showed relatively small improvements in the ‘Inconsistent’ condition (e.g. subjects G.P.P., L.A.H. in Fig. 8) must have large search zones and/or  $H_{\text{opt}}$  approaching  $5.7^\circ$ ; subjects who showed the largest improvements (e.g. E.O., K.C.R.) must have smaller search zones and  $H_{\text{opt}}$  near  $0^\circ$ .

## Discussion

We have shown that performance on a stereo vision task can be improved by artificial disparities that are not possible in nature at the given viewing distance. On-screen vertical disparity is always non-epipolar, that is, geometrically impossible given the current eye position. Adding a constant on-screen vertical disparity is well known to impair performance on tasks involving the detection of horizontal disparity (Duwaer & van den Brink, 1982; Prazdny, 1985; Stevenson & Schor, 1997). Here, we have used on-screen vertical disparity to ‘improve’ performance. To achieve this, on-screen vertical disparity was applied in a very special pattern, so as to mimic the retinal disparity field associated with distant viewing. As a result, our highly contrived artificial stimulus (Fig. 3D) produced better performance than the naturalistic one (Fig. 3B).

We were motivated to produce this stimulus by the theory that stereo correspondence operates with disparity search zones that are fixed in retinotopic coordinates (Schreiber *et al.*, 2001). If search zones are fixed, then stereo vision cannot be optimized simultaneously for all eye postures. Thus, the theory predicts that, at non-optimal eye postures, it should be possible to improve performance on stereo tasks by simulating the eye positions for which stereo vision is optimized. Our confirmation of this signature prediction extends the theory of retinally fixed search zones to changes in convergence angle.

### Position and size of search zones

If search zones are fixed, then their vertical extent must reflect a trade-off between keeping stereo vision functional over a wide range of eye postures, and simplifying the correspondence problem by minimizing the number of false matches. Our results enable us to place an upper bound on the vertical extent of search zones at the eccentricity of the target disk: their vertical standard deviation at approximately  $14^\circ$  eccentricity must be  $< 0.6^\circ$ . This is relatively small, which is why our vertical-disparity manipulations made a measurable difference to performance.

Given that search zones have a relatively limited vertical extent, the vertical disparity on which they are centred becomes important. Away



from the fovea, the expected vertical disparity depends on convergence and hence on viewing distance, so it is not obvious where search zones should be centred vertically. By probing stereo correspondence in the four quadrants at an eccentricity of  $10^\circ$ , we have examined this question. Subjects were better at detecting the target disk when the retinal vertical disparity at its centre was  $0.00^\circ$  than when it was  $0.35^\circ$ . This is a relatively small change in disparity compared with V1 receptive field size at that eccentricity (see next section), so the fact that we observed a significant improvement in performance suggests that search zones must be centred quite near-zero retinal vertical disparity, i.e. that stereo vision is optimized for long viewing distance. To identify the precise viewing distance that is optimal, we would need to repeat our experiment at a range of simulated convergences. With our current data, we can conclude that stereo correspondence is optimized for convergences  $< 5.7^\circ$ , corresponding to viewing distances of  $> 60$  cm.

### Relationship to physiology

As discussed in the Introduction, disparity search zones have a natural physiological interpretation: they must be built, ultimately, from disparity-selective neurons in V1. It has been suggested that the spatial resolution of stereo perception reflects this initial encoding (Banks *et al.*, 2004; Nienborg *et al.*, 2004). It is therefore of interest to compare the disparity search zones estimated from our psychophysical data with disparity tuning in V1. We assume that the disparity search zones at each point in the visual field reflect the distribution of preferred disparities among neurons at that retinotopic location, convolved with the range of non-preferred disparities to which each neuron responds. Suppose, in line with empirical evidence (Cumming, 2002), that the population distribution of preferred disparities is a Gaussian centred vertically on  $V_{\text{cen}}$  and with a vertical SD of  $\sigma_{\text{pop}}$ , while each neuron's disparity tuning surface is also Gaussian, with vertical SD  $\sigma_{\text{nm}}$ . This would result in a disparity search zone that is also a Gaussian, centred on  $V_{\text{cen}}$  and with a vertical SD of  $\sigma_{\text{SZ}} = \sqrt{\sigma_{\text{pop}}^2 + \sigma_{\text{nm}}^2}$ . On theoretical grounds, we expect  $V_{\text{cen}}$  to depend on retinal location,  $V_{\text{cen}} \sim \alpha \eta H_{\text{opt}}$ , where  $H_{\text{opt}}$  is the vergence for which stereo vision is optimized (Read *et al.*, 2009). Our results suggest that  $H_{\text{opt}}$  must be relatively small,  $< 5.7^\circ$ , and thus that  $V_{\text{cen}}$  is close to zero ( $< 0.17^\circ$  at  $14^\circ$  eccentricity, i.e. much less than typical receptive field sizes there).

We can compare the value of  $\sigma_{\text{SZ}}$  estimated from our psychophysical data with the data from V1 physiology. Under the stereo energy model, the disparity tuning surface is simply the cross-correlation of the monocular receptive field (Prince *et al.*, 2002), and  $\sigma_{\text{nm}} = \sigma_{\text{RF}}\sqrt{2}$ , where  $\sigma_{\text{RF}}$  is the SD of each monocular RF. The results of Cumming (2002) show that the disparity tuning surfaces of real neurons depart from the predictions of the original stereo energy model, but Read & Cumming (2004) showed that they can be modelled as the sum of several energy model units. Because this model combines monocular units with the same vertical position on the retina, it leaves the relationship  $\sigma_{\text{nm}} = \sigma_{\text{RF}}\sqrt{2}$  unchanged. One study has estimated  $\sigma_{\text{RF}}$  in human patients with subdural electrodes (Yoshor *et al.*, 2007). The smallest RFs recorded in the vicinity of V1 had a full-width at half-height of  $< 1^\circ$ , corresponding to  $\sigma_{\text{RF}} < 0.4^\circ$ . Estimates of  $\sigma_{\text{RF}}$  are also available from several studies in macaques. From Fig. 7 of Nienborg *et al.* (2004) we estimate the mean  $\sigma_{\text{RF}}$  as  $0.3^\circ$ , the same value as reported by Read & Cumming (2003) for a different set of V1 neurons and similar to the values in Parker & Hawken (1988) and Sceniak *et al.* (1999). Data on  $\sigma_{\text{pop}}$  are only available from Cumming (2002); Fig. 4 of that paper suggests a value of at most  $\sigma_{\text{pop}} = 0.1^\circ$ , probably

less as the error on the measurement is of the same order. This leads to an estimate of  $\sigma_{\text{SZ}}$  from V1 physiology as  $0.44^\circ$ , comfortably within the upper bound estimated from our psychophysical data of  $0.60^\circ$ . These physiology data were collected at relatively small eccentricities (mean  $3.7^\circ$  for Nienborg *et al.*, 2004;  $2\text{--}9^\circ$  for Cumming, 2002,  $0.2\text{--}3.5^\circ$  for Parker & Hawken, 1988), whereas the target in our task has a minimum eccentricity of  $10^\circ$  and extends to  $18^\circ$ . Estimates from larger eccentricities are available from Cavanaugh *et al.* (2002). If we identify our  $\sigma_{\text{RF}}$  with the standard deviation of their centre mechanism,  $w_s$ , and estimate  $w_s$  from the radius of the grating summation field shown in their Fig. 2, we obtain the estimate  $\sigma_{\text{RF}} \sim 0.9^\circ$  at eccentricities in the range  $10\text{--}25^\circ$ , rather larger than the upper bound suggested by our psychophysics experiments.

It has recently been suggested that V1 might not require a range of preferred vertical disparities in order to encode 2D disparity (Read & Cumming, 2006; Read, 2010). In this view,  $\sigma_{\text{pop}} = 0$  and the range of detectable vertical disparities is set purely by  $\sigma_{\text{nm}}$ . Our data are consistent with this possibility.

### Optimization for long viewing distance

We have concluded that stereo search zones are centred near-zero vertical disparity, and thus that stereo correspondence is optimized for long viewing distances. This may appear surprising, given that the prevalent view that 'the primary use for stereopsis is to guide the fine movements of the hands' (McKee *et al.*, 1990). Our conclusion regarding stereo correspondence does, however, agree with other aspects of stereo vision.

Several authors have suggested that the empirical horopter is optimized for a ground plane viewed by a standing observer (Helmholtz, 1925; Breitmeyer *et al.*, 1977; Tyler, 1991; Schreiber *et al.*, 2008), implying optimal viewing distances of the same order as the height of the eyes above the ground. Empirically corresponding points are defined as those that give rise to the same perceived direction, so that if empirically corresponding points in each eye are stimulated in alternation, no movement is perceived. Such points are found to have near-zero vertical disparity, meaning that they can be stimulated by physical objects only when viewed at long distances. Schreiber *et al.* (2008) cite viewing distances of 255, 279 and 90 cm for their three observers, corresponding to convergences of 2.4, 1.3 and  $4.2^\circ$  – all  $< 5.7^\circ$ .

Similarly, though stereoacuity is roughly independent of viewing distance for distances  $> 50$  cm, it is significantly worse at viewing distances less than *c.* 50 cm (Amigo, 1963; Brown *et al.*, 1965; Lit & Finn, 1976; Bradshaw & Glennerster, 2006; though see Wong *et al.*, 2002). This is unlikely to reflect the mechanisms discussed in the present paper, as all these studies used foveal stimuli, for which retinal vertical disparity is near-zero independent of viewing distance, while some used vertical rod stimuli, which present information at a wide range of vertical disparities (Amigo, 1963; Brown *et al.*, 1965; Lit & Finn, 1976). Thus, the impaired stereoacuity at short viewing distance must reflect other factors, e.g. the larger physical convergence.

Regardless, several different lines of evidence are now converging on the conclusion that stereo vision is optimized in a number of ways for long viewing distances. This may reflect the distribution of eye postures adopted during natural viewing, if we spend more time looking into the distance than close-up. It may reflect the challenging nature of distance stereo: disparity scales as the inverse square of viewing distance, so a depth step of, e.g. 1% of the viewing distance is far harder to discriminate if the viewing distance is large than if it is small. Thus, stereo vision may be optimized for the most demanding

situations. This may be significant for designers of stereo content, e.g. computer games, viewed at near distance on a desktop screen.

### Effect of the visual periphery

Previous work has suggested that vertical disparities in the periphery may be more influential than sensed eye position in interpreting horizontal disparity, once the stereo correspondence problem has been solved (Bradshaw *et al.*, 1996). By including our three different surround configurations (None/Same/Different), we investigated whether peripheral vertical disparity has a detectable effect on the initial 'extraction' of horizontal disparity during stereo correspondence. Porrill *et al.* (1999) have shown in simulations that a good estimate of eye position can be obtained from the vertical-disparity pattern of false matches in the periphery, even prior to stereo correspondence. Potentially, therefore, disparity search zones might shift to reflect this purely retinal estimate of eye position. For example, in the 'Consistent'/'Same-surround' condition, the large retinal vertical disparities beyond 20° eccentricity could in principle provide a clue to the highly converged eye posture, which could be used to shift search zones closer to the epipolar vertical disparity. If this occurred, performance in the 'Consistent'/'Same-surround' condition should be less poor relative to the 'Inconsistent'/'Same-surround' condition than in the 'No-surround' condition, where less peripheral information is available. Thus, the signature of this shift would be the finding that  $r_{\text{Con, None}}/r_{\text{Inc, None}}$  was smaller than  $r_{\text{Con, Same}}/r_{\text{Inc, Same}}$ . In fact, however, the reduction in effective correlation between the 'Consistent' and 'Inconsistent' conditions is remarkably constant, independent of whether a surround is present or whether it correctly cues the vertical disparities encountered at the target:  $r_{\text{Con, None}}/r_{\text{Inc, None}} = r_{\text{Con, Same}}/r_{\text{Inc, Same}} = r_{\text{Con, Diff}}/r_{\text{Inc, Diff}}$  (Fig. 8). This suggests that the pattern of disparities in the periphery is not used to shift search zones. Rather, search zones seem stubbornly fixed in retinal coordinates, reflecting neither oculomotor nor retinal information regarding eye position.

Although information in the visual periphery did not affect the relative performance between 'Consistent' and 'Inconsistent' conditions, it clearly did have a significant effect on the overall performance in both conditions. Comparing the 'Same-' vs. 'No-surround' conditions, extending the background beyond 20° eccentricity produced improved performance in 7/8 subjects (Supporting Information Table S1:  $G_{\text{Same}} > G_{\text{None}}$  for all subjects, except K.C.R.). This is surprising, given that the information necessary to perform the task is present only up to an eccentricity of 18°, and available from eccentricities as low as 10°. Comparing the 'Same-' vs. 'Different-surround' conditions reveals that the effect of the surround depends critically on vertical disparities in this peripheral location, not on the additional horizontal disparity information or luminance. Performance is impaired if the vertical disparities in the central and peripheral visual field indicate different eye postures, compared with when vertical disparities are globally consistent with a given eye posture (independent of whether that is the eye posture actually adopted).

It is not always the case that simulating inconsistent eye postures across the visual field will impair performance. Serrano-Pedraza *et al.* (2010) recently showed that simulating inconsistent gaze angles can actually improve performance on a slant discrimination task. In their task, stimulus correlation was always 100%, so achieving stereo correspondence was relatively trivial, and the challenge was interpreting the resultant two-dimensional disparity field so as to judge surface slant. Discontinuities in stimulus vertical disparity apparently aided this process, even if they were impossible in natural viewing. In the present paper, we manipulated stimulus binocular

correlation so that the challenge was to achieve stereo correspondence in the first place. Apparently, stereo correspondence is easier when the vertical-disparity field is globally consistent with a single eye position.

We have argued above that this effect of the visual periphery does not appear to be well described by a shift in search zone location. Rather, we suggest that it may reflect cooperative mechanisms within stereo correspondence, an idea going back to Marr & Poggio (1976). Many previous models have postulated inhibitory and excitatory interactions between sensors tuned to different horizontal disparities, with mutual reinforcement between potential matches representing nearby positions on frontoparallel surfaces, and reciprocal inhibition between matches along the same line of sight (Dev, 1975; Nelson, 1975; Julesz & Chang, 1976; Marr & Poggio, 1976) or with different phase disparities (Read & Cumming, 2007). Suppose that similar interactions occur between potential matches with different vertical disparity, such that matches that are compatible with the same eye postures reinforce each other and inhibit other potential matches that require different eye positions. In the 'Same-surround' condition, then, all the correct matches would reinforce one another, whereas in the 'Different-surround' condition, the correct matches beyond 20° would inhibit the correct matches within 20°, and vice versa. This would make stereo correspondence more difficult to achieve, causing the reduction in effective stimulus correlation.

Previous workers have demonstrated that vertical disparity in the far periphery can have an important effect on depth judgements (Rogers & Bradshaw, 1993). The present work probes the efficiency with which disparities are acquired, rather than how they are converted to metric depth. This paper provides the first evidence that vertical disparity in the far periphery can aid the acquisition of disparities, as well as their calibration.

### Summary

Stereo correspondence is the process of identifying features in one eye that match features in the other eye, because both are images of the same physical object. Previous evidence has suggested that the visual system seeks these matches only within limited disparity search zones, which remain fixed in retinotopic coordinates. Our results show for the first time that search zones are not updated to reflect the changes in binocular geometry that occur when people view objects at different distances. This means that stereo correspondence cannot function optimally for all viewing distances. We have demonstrated that stereo vision is optimized for long viewing distances and that, in consequence, performance at close viewing can be improved by artificial disparities that simulate distant viewing. Physiologically, this suggests that neurons in the primary visual cortex are predominantly tuned to near-zero retinal vertical disparities. We have provided the first psychophysical estimate of the extent of eccentrically located search zones, and shown that this is similar to the receptive field sizes of V1 neurons. Finally, we have provided the first evidence that stereo correspondence itself can be affected by the global consistency of the vertical-disparity field. We suggest this could reflect cooperative interactions between disparity-selective neurons activated by similar eye postures.

### Supporting Information

Additional supporting information may be found in the online version of this article:

Fig. S1. Complete psychophysical data and fits for all eight subjects.

Fig. S2. Relative effective correlation for all eight subjects individually, in the same format as Fig. 7, except that here error-bars show the 68% confidence intervals, corresponding to  $\pm 1$  SEM for a normal distribution.

Table S1. Parameters of the fits shown in Supporting Information Fig. S1 for the individual subjects.

Please note: As a service to our authors and readers, this journal provides supporting information supplied by the authors. Such materials are peer-reviewed and may be re-organized for online delivery, but are not copy-edited or typeset by Wiley-Blackwell. Technical support issues arising from supporting information (other than missing files) should be addressed to the authors.

## Acknowledgements

This work was supported by the EPSRC (Neuroinformatics Doctoral Training Centre studentship to G.P.P.), Royal Society (University Research Fellowship UF041260 to J.C.A.R.) and MRC (New Investigator Award 80154 to J.C.A.R.).

## References

- Amigo, G. (1963) Variation of stereoscopic acuity with observation distance. *J. Opt. Soc. Am.*, **53**, 630–635.
- Banks, M.S., Gepshtein, S. & Landy, M.S. (2004) Why is spatial stereoresolution so low? *J. Neurosci.*, **24**, 2077–2089.
- Blakemore, C. (1970) The range and scope of binocular depth discrimination in man. *J. Physiol.*, **211**, 599–622.
- Bradshaw, M.F. & Glennerster, A. (2006) Stereoscopic acuity and observation distance. *Spat. Vis.*, **19**, 21–36.
- Bradshaw, M.F., Glennerster, A. & Rogers, B.J. (1996) The effect of display size on disparity scaling from differential perspective and vergence cues. *Vision Res.*, **36**, 1255–1264.
- Brainard, D.H. (1997) The psychophysics toolbox. *Spat. Vis.*, **10**, 433–436.
- Breitmeyer, B., Battaglia, F. & Bridge, J. (1977) Existence and implications of a tilted binocular disparity space. *Perception*, **6**, 161–164.
- Brown, J.P., Ogle, K.N. & Reihner, L. (1965) Stereoscopic acuity and observation distance. *Invest. Ophthalmol.*, **4**, 894–900.
- Cavanaugh, J.R., Bair, W. & Movshon, J.A. (2002) Nature and interaction of signals from the receptive field center and surround in macaque V1 neurons. *J. Neurophysiol.*, **88**, 2530–2546.
- Cormack, L.K., Stevenson, S.B. & Schor, C.M. (1991) Interocular correlation, luminance contrast and cyclopean processing. *Vision Res.*, **31**, 2195–2207.
- Cumming, B.G. (2002) An unexpected specialization for horizontal disparity in primate primary visual cortex. *Nature*, **418**, 633–636.
- Dev, P. (1975) Perception of depth surfaces in random-dot stereograms: a neural model. *Int. J. Man Mach. Stud.*, **7**, 511–528.
- Duwaer, A.L. & van den Brink, G. (1982) Detection of vertical disparities. *Vision Res.*, **22**, 467–478.
- van Ee, R. & van Dam, L.C. (2003) The influence of cyclovergence on unconstrained stereoscopic matching. *Vision Res.*, **43**, 307–319.
- Helmholtz, H.v. (1925) *Treatise on Physiological Optics*. Optical Society of America, Rochester, NY.
- Hibbard, P.B. (2007) A statistical model of binocular disparity. *Vis. Cog.*, **15**, 149–165.
- Julesz, B. & Chang, J.J. (1976) Interaction between pools of binocular disparity detectors tuned to different disparities. *Biol. Cybern.*, **22**, 107–119.
- Lit, A. & Finn, J.P. (1976) Variability of depth-discrimination thresholds as a function of observation distance. *J. Opt. Soc. Am.*, **66**, 740–742.
- Liu, Y., Bovik, A.C. & Cormack, L.K. (2008) Disparity statistics in natural scenes. *J. Vis.*, **8**, 19.1–19.14.
- Marr, D. & Poggio, T. (1976) Cooperative computation of stereo disparity. *Science*, **194**, 283–287.
- McKee, S.P., Levi, D.M. & Bowne, S.F. (1990) The imprecision of stereopsis. *Vision Res.*, **30**, 1763–1779.
- Mok, D., Ro, A., Cadera, W., Crawford, J.D. & Vilis, T. (1992) Rotation of listing's plane during vergence. *Vision Res.*, **32**, 2055–2064.
- Nelson, J. (1975) Globality and stereoscopic fusion in binocular vision. *J. Theor. Biol.*, **49**, 1–88.
- Nienborg, H., Bridge, H., Parker, A.J. & Cumming, B.G. (2004) Receptive field size in V1 neurons limits acuity for perceiving disparity modulation. *J. Neurosci.*, **24**, 2065–2076.
- Ohzawa, I. (1998) Mechanisms of stereoscopic vision: the disparity energy model. *Curr. Opin. Neurobiol.*, **8**, 509–515.
- Ohzawa, I., DeAngelis, G.C. & Freeman, R.D. (1990) Stereoscopic depth discrimination in the visual cortex: neurons ideally suited as disparity detectors. *Science*, **249**, 1037–1041.
- Parker, A.J. & Hawken, M.J. (1988) Two-dimensional spatial structure of receptive fields in monkey striate cortex. *J. Opt. Soc. Am. A*, **5**, 598–605.
- Pelli, D.G. (1997) The VideoToolbox software for visual psychophysics: transforming numbers into movies. *Spat. Vis.*, **10**, 437–442.
- Porrill, J., Frisby, J.P., Adams, W.J. & Buckley, D. (1999) Robust and optimal use of information in stereo vision. *Nature*, **397**, 63–66.
- Prazdny, K. (1985) Vertical disparity tolerance in random-dot stereograms. *Bull. Psychon. Soc.*, **23**, 413–414.
- Prince, S.J., Pointon, A.D., Cumming, B.G. & Parker, A.J. (2002) Quantitative analysis of the responses of V1 neurons to horizontal disparity in dynamic random-dot stereograms. *J. Neurophysiol.*, **87**, 191–208.
- Read, J.C.A. (2010) Vertical binocular disparity is encoded implicitly within a model neuronal population tuned to horizontal disparity and orientation. *PLoS Comput. Biol.*, **6**, e1000754.
- Read, J.C.A. & Cumming, B.G. (2003) Testing quantitative models of binocular disparity selectivity in primary visual cortex. *J. Neurophysiol.*, **90**, 2795–2817.
- Read, J.C.A. & Cumming, B.G. (2004) Understanding the cortical specialization for horizontal disparity. *Neural Comput.*, **16**, 1983–2020.
- Read, J.C.A. & Cumming, B.G. (2006) Does visual perception require vertical disparity detectors? *J. Vis.*, **6**, 1323–1355.
- Read, J.C.A. & Cumming, B.G. (2007) Sensors for impossible stimuli may solve the stereo correspondence problem. *Nat. Neurosci.*, **10**, 1322–1328.
- Read, J.C.A., Phillipson, G.P. & Glennerster, A. (2009) Latitude and longitude vertical disparities. *J. Vis.*, **9**, 11.1–11.37.
- Rogers, B.J. & Bradshaw, M.F. (1993) Vertical disparities, differential perspective and binocular stereopsis. *Nature*, **361**, 253–255.
- Sceniak, M.P., Ringach, D.L., Hawken, M.J. & Shapley, R. (1999) Contrast's effect on spatial summation by macaque V1 neurons. *Nat. Neurosci.*, **2**, 733–739.
- Schreiber, K., Crawford, J.D., Fetter, M. & Tweed, D. (2001) The motor side of depth vision. *Nature*, **410**, 819–822.
- Schreiber, K.M., Hillis, J.M., Filippini, H.R., Schor, C.M. & Banks, M.S. (2008) The surface of the empirical horopter. *J. Vis.*, **8**, 7.1–7.20.
- Serrano-Pedraza, I. & Read, J.C.A. (2009) Stereo vision requires an explicit encoding of vertical disparity. *J. Vis.*, **9**, 1–13.
- Serrano-Pedraza, I., Phillipson, G.P. & Read, J.C.A. (2010) A specialization for vertical disparity discontinuities. *J. Vis.*, **10**, 2.
- Stevenson, S.B. & Schor, C.M. (1997) Human stereo matching is not restricted to epipolar lines. *Vision Res.*, **37**, 2717–2723.
- Tweed, D. (1997) Visual-motor optimization in binocular control. *Vision Res.*, **37**, 1939–1951.
- Tyler, C. (1991) The horopter and binocular fusion. In Regan, D. (Ed.), *Binocular Vision*. Macmillan, New York, pp. 19–37.
- Wong, B.P., Woods, R.L. & Peli, E. (2002) Stereoacuity at distance and near. *Optom. Vis. Sci.*, **79**, 771–778.
- Yoshor, D., Bosking, W.H., Ghose, G.M. & Maunsell, J.H. (2007) Receptive fields in human visual cortex mapped with surface electrodes. *Cereb. Cortex*, **17**, 2293–2302.